DOI 10.1007/s10812-019-00762-z
Journal of Applied Spectroscopy, Vol. 85, No. 6, January, 2019 (Russian Original Vol. 85, No. 6, November–December, 2018)

STUDY OF THE IR SPECTRA OF THE SALIVA OF CANCER PATIENTS

L. V. Bel'skaya,[a*] E. A. Sarf,[a] and I. A. Gundyrev[b] UDC 543.422;612.313.1;612.313.6;616006.6

Feasibility has been demonstrated in principle for the diagnosis of lung and breast cancer by subjecting saliva to Fourier transform IR spectroscopy. Statistically significant differences in the saliva of lung cancer patients are seen at 1070–1240 cm^{-1}, while significant differences are seen throughout the entire range for breast cancer patients. The $I_{1398/1454}$ and $I_{1240/1310}$ ratios were determined and found to be statistically reliable for detecting cancer pathology. Correlations were found for the intensities of the absorption bands in these IR spectra with nonspecific biochemical saliva parameters, which generally characterize greater intoxication as well as suppression of the systems for antioxidant protection and the immune response. A promising research trend involves the use of the IR spectroscopy of saliva for monitoring treatment and cancer recurrence.

Keywords: *saliva, Fourier transform IR spectroscopy, oncology, diagnostics.*

Introduction. The identification of specific biomarkers for cancer detection along with the development of reliable and simple methods are important for improving the early diagnosis of cancer and its treatment [1]. A promising method in this area involves the use of Fourier transform IR spectroscopy [2–4]. This method has been described for the detection and monitoring of the treatment of breast cancer [5, 6]. Differences have been shown in the absorption spectra of blood serum from lung cancer patients and healthy individuals [7, 8]. There have been reports in the literature on the diagnosis of cancer of the stomach [9], intestines [10, 11], liver [12], prostate [13, 14], thyroid [15], testicles [16], bladder [17], and other organs [18–20].

Attention is now being focused on saliva as an informative biomaterial for the noninvasive diagnosis and monitoring of the human organism [21, 22]. However, the use of the IR spectroscopy of saliva for cancer diagnosis has not been described in the literature. In the present work, we established the feasibility of using Fourier transform IR spectroscopy of the saliva for the diagnosis of cancer, namely, lung and breast cancer, which are the most common types of cancer for men and women, respectively.

Materials and Methods. Two groups were studied: the major group composed of lung cancer (men) and breast cancer patients (women) and a healthy control group. The major group contained 40 lung cancer patients (16 with squamous cell carcinoma, 16 with adenocarcinoma, and 8 with neuroendocrine tumors) and 50 female breast cancer patients. The control group contained individuals, for whom medical examination did not reveal either lung or breast cancer pathology (55 men and 58 women). The groups were selected in parallel. The criteria for selection were: patient age 30–75 years, no surgical, chemotherapeutic, or radiation treatment at the time of investigation, no sign of active infection including suppuration, oral cavity prophylaxis. The absence of histological verification of the diagnosis was a criterion for exclusion from the study. This research was approved by the Ethics Committee of the Public Health Budget Institution of the Omsk Oblast concerning clinical oncological examination, July 21, 2016, Protocol No. 15.

Saliva (1 mL) was collected from all the participants prior to treatment. The saliva samples were collected in the morning from fasting patients and placed into sterile test tubes, which were centrifuged at 7000 rpm. Then, 50-mL samples were dried on a zinc selenide plate at constant 37°C. The IR absorption spectra were taken on a Simex FT801 Fourier transform IR spectrometer at 500–4000 cm^{-1}.

The statistical analysis of the data was carried out using the StatSoft Statistica 10.0 program by a nonparametric method using the Wilkinson criterion in dependent groups and the Mann–Whitney U-criterion for independent groups.

*To whom correspondence should be addressed.

[a]Omsk State Pedagogical University, 14 Naberezhnaya Tukhachevskogo, Omsk, 644043, Russia; email: ludab2005@mail.ru; [b]TriSoft, Omsk, Russia. Translated from Zhurnal Prikladnoi Spektroskopii, Vol. 85, No. 6, pp. 952–961, November–December, 2018. Original article submitted August 22, 2018.

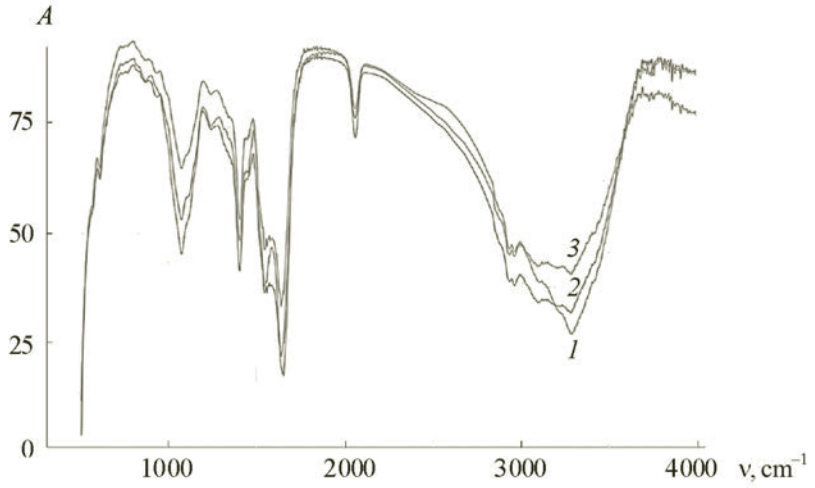

Fig. 1. Averaged IR spectra of saliva: 1) control group, 2) lung cancer, and 3) breast cancer.

Description of the sample selection was carried out by calculating the median (Me) and interquartile range for 25 (LQ) and 75% (UQ). The differences were considered statistically significant for $p < 0.05$.

Results and Discussion. For each group in this study, we calculated the averaged saliva IR spectrum (Fig. 1). The corresponding spectral features for proteins, phospholipids, and nucleic acids can be identified in the saliva IR spectra [23]. Qualitative differences between the spectra in the groups studied were not found but band shifts were discovered (Table 1). The same type of protein group band shifts was found for the patients with lung and breast cancer. Thus, the amide I band in the normal group was found near 1655 cm^{-1} but was shifted in cancer patients to 1640 cm^{-1}, which may be related to a change in the secondary protein structures. Concurrently, the amide II band in the normal group had a maximum at 1547 cm^{-1}, while it was shifted to 1549 cm^{-1} for both major cancer patient groups. The amide III band found in the normal patient group at 1300 cm^{-1} is shifted to 1310 cm^{-1} in the case of lung cancer and 1315 cm^{-1} in the case of breast cancer. Shifts were also found for the bands corresponding to lipids and fatty acids (Table 1). In particular, the carbonyl group band is shifted from 1740 to 1735 cm^{-1}, while the band at 1393 cm^{-1} is shifted to 1406 cm^{-1} for the cancer patients. The band as 1240 cm^{-1} for the phosphodiester group is shifted to 1242 cm^{-1} for the breast cancer patients and 1244 cm^{-1} for the lung cancer patients, while the band at 1075 cm^{-1} for the normal individuals is shifted to 1076–1078 cm^{-1} for both cancer pathologies. In the case of the band in the vicinity of 1240 cm^{-1}, the shift may indicate a greater fraction of hydrogen bonding in the normal individuals, while in the case of the band in the vicinity of 1075 cm^{-1}, the shift may indicate an interaction between the nucleic acids and water. Since both these bands are attributed mainly to the contribution of nucleic acids, these shifts may characterize a change in the nucleic acid structure upon carcinogenesis.

In the next step, we compared the band intensities in the IR spectra of saliva of lung cancer patients, breast cancer patients, and normal individuals (control) (Tables 2 and 3). The lung cancer patient group includes only males. Thus, the control group is also divided into two subgroups relative to gender for a correct evaluation of the results obtained. Statistically reliable differences for the IR spectra of the saliva of the lung cancer patients are seen in bands in the range 1070–1240 cm^{-1}. The bands in this range can be assigned to nucleic acids [24].

Saliva is known to contain extracellular DNA, while genomic analysis shows that 70% of the saliva DNA originates from blood plasma, while 30% comes from the oral microbiota [25]. The content of free (extracellular) nucleic acids in human blood plasma and, hence, in saliva, is elevated in some pathological processes such as cancer, inflammation, and trauma [26]. Thus, DNA fragments originating from tumor cells, "tumor" mRNA, and microRNA are detected in the blood of cancer patients [27, 28]. The presence of circulating DNA in the blood of both healthy individuals and cancer patients is attributed to cell decomposition (apoptosis and necrosis) and cellular secretion [29]. Cell decomposition leads to the liberation of the cell contents, fragmentation of molecules, and the phagocytosis of these molecules. Tumor cells circulating in the blood stream may also contribute to the pool of extracellular molecules [30]. Normal cells have been shown to undergo, as a rule, an ordered apoptosis process with the formation and entry into the blood stream of discrete fragments of predominantly

TABLE 1. Major Absorption Bands (ν, cm^{-1}) in the IR Spectra of Saliva in the Groups Studied

Control	Lung cancer	Breast cancer	Type of vibration
3283–3285	3282	3282	νNH
3065	3070	3070	R-NH_2 (ν_{as}NH, ν_sNH) R-NH (νNH)
2961–2963	2963	2959	$\nu_{as}CH_3$
2934	2934–2936	2934	$\nu_{as}CH_2$
2875	2876	2876	ν_sCH_3
2850	2855	2855	ν_sCH_2
2059	2060	2060	νSCN^-
1740	1735	1736	νC=O
1655	1640	1640	νCO
1547	1549	1549	δNH, νCN
1452	1460	1460	δCH_2
1393	1406	1406	δCH_3
1300	1310	1315	δNH, νCN
1240	1244	1242	$\nu_{as}PO$
1160–1165	1160	1155	νCO, νCC
1121	1120	1120	ν_sPO, νCC, νCO
1075	1076–1078	1078	νCN, $\nu_sPO_2^-$
955–960	960	970	νCC, νCO, νCH_2OH
925–935	929–931	929–933	νCC, νCO, νCH_2OH
860	860	860	νPO (P_2O_7), δOCN, δNH
613–615	613–615	613	δCO

mononucleosome dimensions (~150 base pairs), while necrosis is more characteristic for tumor cells. The DNA formed in this case is heterogeneous and composed of 200–400 base pairs [28]. Depending on the stage of the disease and, thus, the size of the tumor, the fraction of "tumor" DNA varies in a broad range from 3 to 93% of the total mass of circulating DNA [31].

The differences in the spectra are much greater for the breast cancer patients (Table 3). The vibrations of the phosphodiester groups, nucleic acids, and phospholipids found between 1300 and 800 cm^{-1} are useful biomarkers for cancer detection [32]. The band at 970 cm^{-1}, which describes protein phosphorylation processes as well as the content of cellular DNA, can be used to characterize cellular activity, for example, in cancer progression [33]. Vibrations of methyl and methylene groups of proteins and lipids as well as of the carboxyl groups of fatty acids and amino acids can be detected at 1500–1300 cm^{-1} [34]. The bands at 1700–1580 cm^{-1} may characterize DNA and RNA as well as providing information on changes in the conformational structure of proteins [35, 36]. The bands at 1740–1710 cm^{-1} are mainly ascribed to the absorption of phospholipids but the band at 1714 cm^{-1} may be assigned to the absorption of nucleic acids, which may be used a prognosis marker, especially for leukemia [37]. The range from 3050 to 2800 cm^{-1}, which contains vibrational bands for the methyl and methylene groups of saturated and unsaturated alkyl chains, may prove useful for evaluating the permeability of cell membranes as well as processes involving oxidative modification of proteins [38].

We should note that in the entire spectral range, the band intensity in the case of both breast and lung cancer is lower than for the control group (Tables 2 and 3). An exception is found for the range 2800–3050 cm^{-1}, which may be related to more pronounced peroxy oxidation of cell membrane lipids and an increase in the endogenous intoxication in the case of cancer pathology.

These results are supported by the use of multidimensional statistical methods, in particular, discriminant analysis (Fig. 2). The diagram for the scatter of canonical values shows that the points corresponding to the control group samples are located to the left of the vertical 0–0 axis, while the points corresponding to the breast and lung cancer patients are on

TABLE 2. Absorption Band Intensities in the Spectra of Healthy Males and Lung Cancer Patients

ν, cm^{-1}	Control (M), $n = 55$	Lung cancer, $n = 40$	p
613–615	35.3 [29.0; 41.0]	35.6 [31.6; 41.7]	0.5273
860	11.5 [6.4; 18.3]	11.4 [6.1; 19.0]	0.8042
925–935	14.9 [9.3; 22.5]	16.7 [8.0; 21.9]	0.9638
960–970	18.3 [14.3; 26.1]	16.5 [10.0; 23.5]	0.0972
1070–1080	57.2 [44.8; 65.6]	44.2 [35.5; 54.7]	**0.0007***
1120–1130	46.4 [37.2; 53.4]	37.4 [29.6; 49.4]	**0.0060***
1155–1165	34.7 [28.4; 41.9]	28.7 [22.8; 38.1]	**0.0152***
1240	26.6 [20.8; 32.6]	21.6 [16.4; 30.4]	**0.0447***
1310	26.4 [21.4; 32.7]	24.1 [19.1; 34.2]	0.2564
1400	52.9 [45.3; 67.5]	58.4 [47.6; 69.3]	0.8150
1460	36.2 [29.4; 47.2]	33.0 [25.4; 43.8]	0.1153
1550	70.5 [56.7; 79.9]	62.7 [55.0; 76.1]	0.1678
1640	93.9 [78.2; 97.2]	83.5 [63.5; 98.9]	0.2653
1735	17.5 [10.3; 22.3]	13.2 [9.8; 19.4]	0.1834
2060	23.6 [13.4; 36.9]	19.4 [12.8; 28.6]	0.2337
2850	44.2 [34.8; 52.9]	47.1 [37.0; 58.4]	0.5365
2875	47.9 [36.7; 55.5]	50.7 [38.7; 62.9]	0.4784
2930	58.5 [45.2; 66.9]	61.9 [49.0; 73.0]	0.5365
2950	59.3 [46.9; 68.0]	62.1 [50.3; 74.5]	0.5319
3070	65.7 [49.7; 75.5]	66.4 [54.4; 78.8]	0.8751
3266	82.1 [64.9; 87.8]	72.6 [43.3; 88.1]	0.1185
3280	83.4 [65.8; 89.1]	72.9 [43.8; 89.1]	0.0958

*The differences are statistically significant, $p < 0.05$.

the right. A sharp delineation relative to the horizontal axis was not noted, which apparently is due to changes in the human organism common for these groups in the case of cancer pathology.

Additional diagnostic significance may be found not only in the absorption intensities at specific wavelengths but also in the ratio of the intensities of individual bands. Thus, the intensity ratio of bands 2955/2921 cm^{-1}, which shows the ratio of branched and unbranched lipid and fatty acid molecules (CH_3/CH_2), may hold significant information. In the case of cancer pathology, this ratio is lower than in the norm [12], which indicates a less branched chain and/or longer chains of the lipids and fatty acids in comparison with the norm. The ratio of the intensities of the bands 1744/1082 cm^{-1} may represent the lipids/nucleic acids and fatty acids/nucleic acids ratios. The greater ratio in the case of cancer indicates that the content of lipids and fatty acids is elevated in comparison with nucleic acids. The intensity ratio of bands 1640/1535 cm^{-1} may be used to reflect changes in the secondary protein structure and processes involved in the breakdown of hypomethylation [36]. Wang et al. [7] compared cancerous and noncancerous lung tissue using Fourier transform IR spectroscopy and discovered four intensity ratios $I_{1640/1550}$, $I_{1460/1400}$, $I_{1240/1310}$, and $I_{1080/1160}$ useful for identifying malignant and healthy tissues.

We have shown a consistent change in the band intensity ratios for both groups in going from healthy volunteers to cancer patients (Tables 4 and 5). Thus, the $I_{1398/1454}$ ratio reliably increases in this case. This is a ratio of the intensity of the bands for the methylene groups of amino acid sidechains (1398 cm^{-1}) and the sidechains of amino acids in proteins and lipids (1454 cm^{-1}). The $I_{1460/1400}$ ratio is a value inverse to the $I_{1398/1454}$ ratio and thus, decreases consistently in going from the control group to the major cancer patient group. The $I_{1240/1310}$ ratio decreases consistently. The decrease in the intensity of the phospholipid band (1240 cm^{-1}) is more pronounced than for amide III (1310 cm^{-1}). The decrease in the $I_{1640/1535}$ ratio,

TABLE 3. Absorption Band Intensities in the Spectra of Healthy Women and Breast Cancer Patients

ν, cm^{-1}	Control (F), $n = 58$	Breast cancer, $n = 50$	p
613–615	35.9 [31.8; 42.8]	33.1 [29.8; 36.8]	**0.0316***
860	9.8 [5.6; 19.1]	5.4 [3.2; 11.5]	**0.0083***
925–935	14.6 [7.6; 20.1]	10.0 [4.7; 16.2]	**0.0430***
960–970	17.9 [12.1; 23.8]	9.3 [6.8; 17.5]	**0.0001***
1070–1080	52.3 [42.9; 63.9]	31.7 [22.7; 42.9]	**0.0000***
1120–1130	41.9 [33.6; 48.8]	28.1 [19.0; 37.3]	**0.0000***
1155–1165	32.4 [25.3; 38.4]	20.7 [14.0; 29.6]	**0.0000***
1240	23.4 [18.6; 28.3]	14.9 [9.8; 22.6]	**0.0000***
1310	21.8 [18.2; 27.9]	17.9 [11.4; 25.8]	**0.0050***
1400	44.6 [36.8; 56.4]	44.8 [28.9; 60.7]	0.4957
1460	31.2 [25.9; 37.5]	24.2 [15.7; 31.2]	**0.0013***
1550	60.6 [48.2; 68.3]	50.7 [37.5; 70.6]	0.1956
1640	86.6 [61.2; 96.8]	62.7 [43.4; 84.3]	**0.0008***
1735	13.8 [9.5; 18.9]	9.6 [7.6; 13.3]	**0.0009***
2060	23.6 [12.8; 32.8]	16.1 [11.5; 25.2]	**0.0410***
2850	38.0 [28.6; 47.9]	40.8 [30.7; 54.9]	0.2009
2875	39.6 [29.9; 50.4]	41.9 [31.3; 58.1]	0.2492
2930	49.2 [38.6; 60.6]	52.9 [36.5; 69.3]	0.3823
2950	49.9 [38.8; 62.3]	52.8 [36.3; 70.4]	0.4704
3070	55.2 [41.9; 68.7]	54.1 [38.4; 72.0]	0.8060
3266	73.9 [50.9; 85.9]	53.6 [42.3; 72.0]	**0.0047***
3280	75.3 [52.1; 87.3]	54.3 [42.8; 72.9]	**0.0035***

which characterizes the intensities of the amide I and amide II bands, is also statistically reliable for the breast cancer patients (Table 5).

We then compared the ratios at different stages of the disease (Tables 6 and 7). For both pathologies, it is difficult to establish unequivocal change in the parameters studied. Thus, the band intensity ratio 2955/2921 cm^{-1} decreases steadily in breast cancer patients in going from local involvement to metastasis, reaching a minimum for metastatic disease, while the minimum value of this ratio for lung cancer patients is found in the $T_1N_{0–3}M_0$ stage.

On the whole, we note that the greatest difference in the ratios from the control group in the case of breast cancer is observed in the initial stages of the disease (Fig. 3a), while the greatest differences in the case of lung cancer are found in advanced stages (Fig. 3b). Statistically significant differences between the disease stages were found only for breast cancer. The lack of unequivocal dynamics of these ratios in the lung cancer group may be related to the heterogeneity of the group, which combines patients with several histological types of this disease. However, the small size of the sample does not permit a proper statistical comparison of the various histological types and stages. Such a correlation would require further research.

The patterns found for the change in the ratios may be attributed to the corresponding changes in the biochemical saliva content for the pathologies studied. Thus, the lung cancer patient group showed a correlation of the $I_{1398/1454}$ ratio with the lipoperoxidase indices (conjugated dienes, $r = –0.3856$) and endogenous intoxication ($r = –0.3608$). Similarly, a significant correlation interrelationship was found for the ratio $I_{1240/1310}$ with lipoperoxidase indices (conjugated trienes, $r = 0.4176$), endogenous intoxication ($r = 0.3563$), and also with catalase activity ($r = 0.3416$) and the sialic acid concentration ($r = 0.4176$). In previous work [40], we showed that the content of the primary lipoperoxidation products (diene conjugates) is lower in the saliva of lung cancer patients, while the level of secondary products increases. The insufficient level of

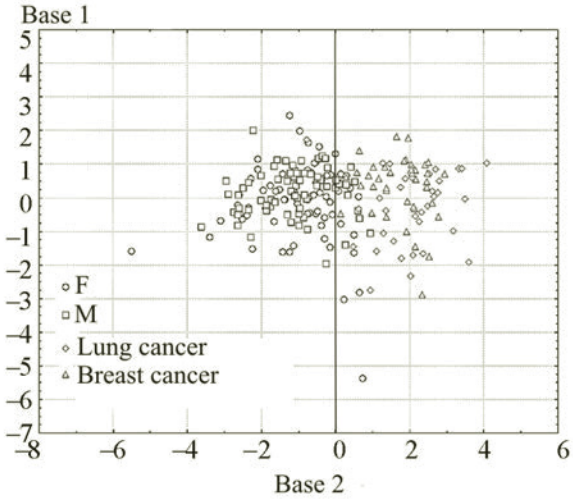

Fig. 2. Diagram for the scatter of canonical values for the groups studied.

TABLE 4. Intensity Ratios in the Spectra of Healthy Males and Lung Cancer Patients

Intensity ratio	Control (M), $n = 55$	Lung cancer, $n = 40$	p	±Δ, %
$I_{2955/2921}$	1.016 [1.008; 1.026]	1.017 [1.002; 1.026]	0.6175	+0.1
$I_{1744/1082}$	0.314 [0.213; 0.390]	0.321 [0.254; 0.455]	0.2806	+2.2
$I_{1640/1535}$	1.276 [1.168; 1.423]	1.247 [1.138; 1.340]	0.4280	–2.3
$I_{1398/1454}$	1.541 [1.339; 1.726]	1.743 [1.458; 1.946]	**0.0060***	+13.1
$I_{1460/1400}$	0.649 [0.579; 0.747]	0.574 [0.514; 0.686]	**0.0060***	–11.6
$I_{1240/1310}$	1.004 [0.936; 1.044]	0.887 [0.832; 0.954]	**0.0000***	–11.7
$I_{1080/1160}$	1.554 [1.365; 1.833]	1.514 [1.409; 1.669]	0.5692	–2.6

TABLE 5. Intensity Ratios in the Absorption Spectra of Healthy Women and Breast Cancer Patients

Intensity ratio	Control (F), $n = 58$	Breast cancer, $n = 50$	p	±Δ, %
$I_{2955/2921}$	1.013 [0.999; 1.020]	1.006 [0.990; 1.022]	0.2451	–0.7
$I_{1744/1082}$	0.272 [0.202; 0.427]	0.309 [0.230; 0.452]	0.1468	+13.6
$I_{1640/1535}$	1.351 [1.227; 1.521]	1.184 [1.124; 1.317]	**0.0001***	–12.4
$I_{1398/1454}$	1.417 [1.252; 1.740]	1.786 [1.591; 1.991]	**0.0000***	+26.0
$I_{1460/1400}$	0.706 [0.575; 0.799]	0.560 [0.502; 0.629]	**0.0000***	–20.7
$I_{1240/1310}$	1.013 [0.968; 1.061]	0.887 [0.825; 0.955]	**0.0000***	–12.4
$I_{1080/1160}$	1.614 [1.457; 1.834]	1.584 [1.430; 1.730]	0.2751	–1.9

primary lipoperoxidation products may be a consequence of the resistance of tumor tissue to the peroxide stress initiators and modified functioning of the enzyme systems regulating the peroxy oxidation of lipids. The level of secondary products in the case of lung cancer is elevated, perhaps as a response to the more toxic metabolites released from the cells. The activity of the catalase, which is the first line of defense against free radical oxidation, is considerably lower in the case of lung cancer. This finding is also in accord with decrease in the $I_{1240/1310}$ ratio, which correlates with this activity. A decrease is found in the sialic acid concentration in the case of lung cancer, which is more pronounced in advances stages of the disease and upon spread of the cancer [41].

TABLE 6. Intensity Ratios in the Spectra of Saliva of Patients with Various Stages of Breast Cancer

Intensity ratio	$T_1N_{0–2}M_0$, n = 16	$T_2N_{0–2}M_0$, n = 10	$T_{3-4}N_{0–2}M_0$, n = 14	$T_{1–4}N_{0–2}M_1$, n = 10
$I_{2955/2921}$	1.008 [0.997; 1.023]	1.002 [0.990; 1.027]	1.000 [0.978; 1.020]	0.972 [0.971; 1.018]
$I_{1744/1082}$	0.282 [0.231; 0.354] –	0.366 [0.228; 0.450] –	0.533 [0.392; 0.689] p = 0.0472	0.267 [0.185; 0.437] –
$I_{1640/1535}$	1.158 [1.093; 1.272] –	1.257 [1.139; 1.353] –	1.193 [1.121; 1.248] –	1.317 [1.253; 1.373] p = 0.0390
$I_{1398/1454}$	1.915 [1.703; 2.040] –	1.800 [1.697; 2.087] –	1.644 [1.515; 1.824] p = 0.0082	1.573 [1.343; 1.727] p = 0.0166
$I_{1460/1400}$	0.522 [0.490; 0.589] –	0.556 [0.479; 0.589] –	0.610 [0.549; 0.660] p = 0.0081	0.636 [0.579; 0.745] p = 0.0162
$I_{1240/1310}$	0.848 [0.770; 0.902] –	0.875 [0.831; 0.981] –	0.883 [0.827; 0.910] –	0.980 [0.974; 0.987] p = 0.0030
$I_{1080/1160}$	1.552 [1.472; 1.767]	1.609 [1.386; 1.675]	1.630 [1.417; 1.752]	1.473 [1.288; 1.573]

Note: p) is a statistically significant difference in comparison with the control.

TABLE 7. Intensity Ratios in the Spectra of Saliva of Patients with Various Stages of Lung Cancer

Intensity ratio	$T_1N_{0–3}M_0$, n = 8	$T_2N_{0–3}M_0$, n = 12	$T_{3–4}N_{0–3}M_0$, n = 10	$T_{1–4}N_{0–3}M_1$, n = 10
$I_{2955/2921}$	1.008 [1.001; 1.019]	1.025 [1.004; 1.029]	1.021 [1.005; 1.027]	1.015 [0.995; 1.023]
$I_{1744/1082}$	0.395 [0.303; 0.556]	0.262 [0.198; 0.354]	0.319 [0.250; 0.436]	0.467 [0.293; 0.509]
$I_{1640/1535}$	1.128 [0.974; 1.160]	1.318 [1.273; 1.524]	1.275 [1.215; 1.464]	1.190 [1.012; 1.273]
$I_{1398/1454}$	1.474 [1.219; 2.033]	1.629 [1.369; 1.810]	1.904 [1.705; 1.993]	1.775 [1.640; 1.933]
$I_{1460/1400}$	0.689 [0.509; 0.823]	0.618 [0.553; 0.730]	0.525 [0.502; 0.587]	0.565 [0.517; 0.610]
$I_{1240/1310}$	0.943 [0.771; 0.975]	0.943 [0.865; 0.987]	0.832 [0.827; 0.910]	0.872 [0.845; 0.917]
$I_{1080/1160}$	1.405 [1.304; 1.602]	1.521 [1.410; 1.731]	1.588 [1.472; 1.797]	1.520 [1.253; 1.553]

Note: p) statistically significant difference in comparison with the control.

Correlations were found for the breast cancer group for the $I_{1640/1535}$ and $I_{1240/1310}$ ratios with the conjugated diene content (r = 0.3261 and 0.3364) and parameters of endogenous intoxication (r = 0.5448 and 0.6487). We should also note the significant correlation between the $I_{1240/1310}$ ratio and the saliva arginase activity, which is in accord with the finding of a statistically significant elevation of the activity of this enzyme for the breast cancer group. A correlation was found of xanthine oxidase activity and the $I_{1640/1535}$ ratio. The increased activity of xanthine oxidase indicates enhanced generation of active forms of oxygen and its increased superoxideforming and carcinogenic activity. This effect is more pronounced for the breast cancer patients. A negative correlation was found for the $I_{1398/1454}$ ratio with the total antioxidant activity of saliva (r = –0.3084) as well as the total immunoglobulin content (r = –0.3161), which indicates suppression of the antioxidant protection system in the case of cancer pathology. The $I_{1640/1535}$ ratio demonstrates a negative correlation with the Interleukin2 (IL2) (r = –0.5794) and IL4 (r = –0.3994). The $I_{1240/1310}$ ratio has a negative correlation with IL2 (r = –0.3148) and IL18 (r = –0.3052), while the $I_{1393/1454}$ ratio has a negative correlation with IL6 (r = –0.4286). IL2 produces an immune response and activates factors participating in antiviral, antibacterial, and antitumor protection. IL4 corresponds to a humoral immune response, has local antitumor activity, suppresses the production of inflammation cytokines, and regulates a variety of biological processes such as proliferation, differentiation, and apoptosis in different types of cells. The contents of both IL2 and IL4 are elevated for the breast cancer patients, which is in accord with the decreased $I_{1640/1535}$ and $I_{1240/1310}$ ratios

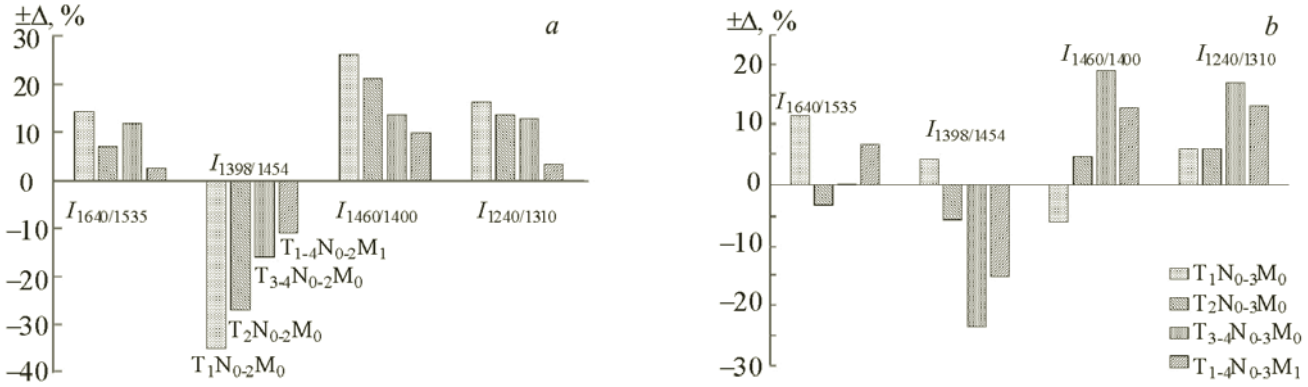

Fig. 3. Relative change in the band intensity ratios for breast (a) and lung cancer patients (b).

(Table 5). IL6 plays a key role in the development of inflammation and an immune response to infection or tissue damage. There is a statistically significant elevation of IL6 in the advanced stages of disease, which may correlate with the decrease in the $I_{1398/1454}$ ratio in going from stage $T_1N_{0–2}M_0$ to stage $T_{1–4}N_{0–2}M_1$ (Table 6).

Thus, correlations are found for the band intensities in the IR spectra and their combinations with unspecific biochemical saliva parameters, which, in general, characterize greater intoxication as well as suppression of the antioxidant protection and the body's immune response. This finding limits the usefulness of these ratios for clinical laboratory diagnosis. The inclusion of only two types of cancer and the small patient sample also hinder drawing conclusions from this study. In the future, we plan to develop a classifying system based on these data using various methods such as linear discriminant analysis, naïve Bayes classifier, support vector method (SVM), gradient boosting method (GBM), random forest, and the method of *k* nearest neighbors as well as evaluate the indices of diagnostic sensitivity and the specificity of the ratios discovered by the cross validation method. In our view, the evaluation of the feasibility of using the IR spectroscopy of saliva holds promise for monitoring the treatment of cancer and as a control for recurrence.

Conclusions. Feasibility in principle has been shown for the diagnosis of lung and breast cancer using Fourier transform IR spectroscopy. Statistically significant differences for the IR spectra of the saliva of lung cancer patients are observed at 1070–1240 cm^{-1}, while such differences are observed for breast cancer patients in the entire spectral range studied. Change in the $I_{1398/1454}$ and $I_{1240/1310}$ ratios is statistically significant for cancer pathology. The greatest difference in these ratios in the case of breast cancer is noted in the early stages of disease, while the greatest difference in the case of lung cancer is observed in advanced stages. These findings may hold promise for the diagnosis of breast cancer in its early stages.

REFERENCES

1. A. J. Atkinson, Jr., W. A. Colburn, V. B. DeGruttola, D. L. DeMets, G. J. Downing, D. F. Hoth, J. A. Oates, C. C. Peck, R. T. Schooley, B. A. Spilker, J. Woodcock, and S. L. Zeger, *Clin. Pharmacol. Ther.*, **69**, 89–95 (2001).
2. G. M. Zubareva, V. M. Minkin, G. Ye. Bordina, I. A. Belyaeva, N. P. Lopina, S. M. Zubarev, and A. V. Kargapolov, *Stomatologiya*, **5**, 7–10 (2009).
3. P. Seredin, D. Goloshchapov, V. Kashkarov, Y. Ippolitov, and K. Bambery, *Results in Physics*, **6**, 315–321 (2016).
4. A. A. Bunaciu, Ş. Fleschin, and H. Y. AboulEnein, *Rev. Roum. Chim.*, **60**, Nos. 5–6, 415–426 (2015).
5. F. Elmi, A. F. Movaghar, M. M. Elmi, H. Alinezhad, and N. Nikbakhsh, *Spectrochim. Acta, A: Mol. Biomol. Spectrosc.*, **187**, 87–91 (2017).
6. J. Depciuch, E. Kaznowska, S. Golowski, A. Koziorowska, I. Zawlik, M. Cholewa, K. Szmuc, and J. Cebulski, *J. Pharm. Biomed. Anal.*, **143**, 261–268 (2017).
7. X. Wang, X. Shen, D. Sheng, X. Chen, and X. Liu, *Spectrochim. Acta, A: Mol. Biomol. Spectrosc.*, **122**, 193–197 (2014).
8. X. Sun, J. Xu, Y. Zhang, and K. Sun, *J. Surg. Res.*, **179**, 33–38 (2013).
9. D. Sheng, Y. Wu, X. Wang, D. Huang, X. Chen, and X. Liu, *Spectrochim. Acta, A: Mol. Biomol. Spectrosc.*, **116**, 365–369 (2013).

10. E. Kaznowska, J. Depciuch, K. Szmuc, and J. Cebulski, *J. Pharm. Biomed. Anal.*, **134**, 259–268 (2017).
11. L. Dong, X. J. Sun, Z. Chao, S. Y. Zhang, J. B. Zheng, R. Gurung, J. K. Du, J. S. Shi, Y. F. Zhang, and J. G. Wu, *Spectrochim. Acta A*, **122**, 288–294 (2014).
12. D. Sheng, F. Xu, Q. Yu, T. Fang, J. Xia, S. Li, and X. Wang, *J. Mol. Struct.*, **1099**, 18–23 (2015).
13. M. J. Baker, E. Gazi, M. D. Brown, J. H. Shanks, N. W. Clarke, and P. Gardner, *J. Biophoton.*, **2**, 104–113 (2009).
14. E. Gazi, M. Baker, J. Dwyer, N. P. Lockyer, P. Gardner, J. H. Shanks, R. S. Reeve, C. A. Hart, N. W. Clarke, and M. D. Brown, *Eur. Urology*, **50**, 750–761 (2006).
15. Y. Liu, Y. Xu, Y. Liu, Y. Zhang, D. Wang, D. Xiu, Z. Xu, X. Zhou, J. Wu, and X. Ling, *Brit. J. Surg.*, **98**, 380–384 (2011).
16. K. Gajjar, J. Trevisan, G. Owens, P. J. Keating, N. J. Wood, H. F. Stringfellow, P. L. MartinHirsch, and F. L. Martin, *Analyst*, **138**, 3917–3926 (2013).
17. J. Ollesch, M. Heinze, H. M. Heisse, T. Behrens, T. Brüning, and K. Gerwert, *J. Biophotonics*, **7**, 216–221 (2014).
18. X. Q. Zhang, Z. Xu, X. F. Ling, Y. Z. Xu, and J. G. Wu, *Spectrosc. Spect. Anal.*, **30**, 30–34 (2010).
19. J. Trevisan, P. P. Angelov, P. L. Carmichael, A. D. Scott, and F. L. Martin, *Analyst*, **137**, 3202–3215 (2012).
20. J. G. Kelly, M. N. Singh, H. F. Stringfellow, M. J. Walsh, J. M. Nicholson, F. Bahrami, K. M. Ashton, M. A. Pitt, P. L. MartinHirsch, and F. L. Martin, *Cancer Lett.*, **274**, 208–217 (2009).
21. P. C. Caetano Júnior, J. FerreiraStrixino, and L. Raniero, Res. Biomed. Eng., **31**, 116–124 (2015).
22. L. M. Rodrigues, T. D. Magrini, C. F. Lima, J. Scholz, H. da Silva Martinho, and J. D. Almeida, *Spectrochim. Acta, A: Mol. Biomol. Spectrosc.*, **174**, 124–129 (2017).
23. L. B. Bel'skaya, E. A. Sarf, and N. A. Makarova, *Zh. Prikl. Spektrosk.*, **85**, No. 3, 436–442 (2018) [*J. Appl. Spectrosc.*, **85**, No. 3, 445–451 (2018)].
24. E. Bogomolny, S. Argov, S. Mordechai, and M. Huleihel, *Biochim. Biophys. Acta*, **1780**, No. 9, 1038–1042 (2008).
25. T. Nonaka and D. T. W. Wong, *The Enzymes*, **42**, 125–151 (2017).
26. V. N. Kondratova, I. V. Botezatu, V. P. Shelepov, and A. V. Likhtenshteyn, *Ros. Bioterapevt. Zh.*, **12**, No. 3, 3–10 (2013).
27. V. Garcia, J. M. Garcia, C. Pena, J. Silva, G. Domínguez, V. Lorenzo, R. Diaz, P. Espinosa, J. G. de Sola, B. Cantos, and F. Bonilla, *Cancer Lett.*, **263**, 312–320 (2008).
28. N. Miura, H. Nakamura, R. Sato, T. Tsukamoto, T. Harada, S. Takahashi, Y. Adachi, K. Shomori, A. Sano, Y. Kishimoto, H. Ito, J. Hasegawa, and G. Shiota, *Cancer Sci.*, **97**, 1366–1373 (2006).
29. M. Stroun, P. Maurice, V. Vasioukhin, J. Lyautey, C. Lederrey, F. Lefort, A. Rossier, X. Q. Chen, and P. Anker, *Ann. N. Y. Acad. Sci.*, **906**, 161–168 (2000).
30. H. Schwarzenbach, C.AlixPanabieres, I. Muller, N. Letang, J. P. Vendrelli, X. Rebillard, and K. Pantel, *Clin. Cancer Res.*, **15**, 1032–1038 (2009).
31. G. Jian, Z. Songwen, Z. Ling, D. Qinfang, Z. Jie, T. Liang, and Z. Caicun, *J. Cancer Res. Clin. Oncol.*, **136**, 1341–1346 (2010).
32. G. I. Dovbeshko, V. I. Chegel, N. Y. Gridina, O. P. Repnytska, Y. M. Shirshov, V. P. Tryndiak, I. M. Todor, and G. I. Solyanik, *Biopolymers*, **67**, No. 6, 470–486 (2002).
33. S. Argov, R. K. Sahu, E. Bernshtain, A. Salam, G. Shohat, U. Zelig, and S. Mordechai, *Biopolymers*, **75**, No. 5, 384–392 (2004).
34. Y. Yang, J. SuleSuso, G. D. Sockalingum, G. Kegelaer, M. Manfait, and A. J. El Haj, *Biopolymers*, **78**, No. 6, 311–317 (2005).
35. Q. B. Li, X. J. Sun, Y. Z. Xu, L. M. Yang, Y. F. Zhang, S. F. Weng, and J. S. Shi, *Clin. Chem.*, **51**, No. 2, 346–350 (2005).
36. Z. Ganim, H. S. Chung, A. W. Smith, L. P. Deflores, K. C. Jones, and A. Tokmakoff, *Acc. Chem. Res.*, **41**, No. 3, 432–441 (2008).
37. C. P. Schultz, *Technol. Cancer Res. Treatment*, **1**, No. 2, 95–104 (2002).
38. C. Petibois and G. Deleris, *Trends Biotechnol.*, **24**, No. 10, 455–462 (2006).
39. S. Zhou, Z. Xu, X. F. Ling, Q. B. Li, Y. Z. Xu, L. Zhang, H. M. Zhao, L. X. Wang, K. Y. Hou, X. S. Zhou, and J. G. Wu, *Chin. J. Oncol.*, **28**, No. 7, 512–514 (2006).
40. L. V. Bel'skaya, V. K. Kosenok, and Zh. Massard, *Diagnostics*, **6**, No. 4, 39 (2016).
41. L. V. Bel'skaya, V. K. Kosenok, and Zh. Massard, *Sovrem. Tekhnol. Med.*, **10**, No. 2, 110–117 (2018).